
Numerical investigation of unsteady buoyancy driven indoor air flow characteristics under various range of internal heat generation

V.R. Lenin*

Department of Mechanical Engineering,
Mahendra Institute of Engineering and Technology,
Namakkal – 637503, Tamilnadu, India
Email: leninrangasamy@gmail.com
*Corresponding author

S. Sivalakshmi

Department of Mechanical Engineering,
Government College of Engineering – Salem,
Salem – 636011, Tamilnadu, India
Email: sivalakshmit@gmail.com

Abstract: Increase in global warming raises the cooling load to all kinds of building sector. Buildings consume more energy for cooling or heating and it depends on the regional climatic conditions. In summer region, peoples are paying more interest in implementing cooling technique or equipment to achieve the comfort environment. Before analysing the building nature implementation of any machinery leads further increase in energy demand also comfort environment may not be possible. In this work the maximum indoor air temperature of a closed room was investigated under transient condition with various range of internal heat flux. The three dimensional isolated room with constant thermal boundary condition was modelled and the grid independence study executed. The result shows that the flow pattern of the room with hot wall and without hot walls varies. Machinery or equipment selection for cooling of the building plays the important role in the view of efficient utilisation.

Keywords: transient condition; computational fluid dynamics; CFD; indoor air temperature; internal heat flux; indoor air flow profile; buoyancy effect; indoor environment; building simulation; numerical investigation; comfort environment; hot walls.

Reference to this paper should be made as follows: Lenin, V.R. and Sivalakshmi, S. (2018) 'Numerical investigation of unsteady buoyancy driven indoor air flow characteristics under various range of internal heat generation', *Int. J. Environment and Sustainable Development*, Vol. 17, Nos. 2/3, pp.295–315.

Biographical notes: V.R. Lenin is working as an Assistant Professor of Mechanical Engineering at the Mahendra Institute of Engineering and Technology, Namakkal, Tamilnadu, India. He acquired both his Bachelor's and Master's degree in Mechanical Engineering from the Anna University. His research interest includes enhancing heat transfer, convective heat transfer, building simulation, building cooling, renewable and sustainable energy resources.

S. Sivalakshmi is working as an Assistant Professor in Mechanical Engineering at the Government College of Engineering where she has been a faculty member since 2006. She completed her PhD at the Anna University and her BE in Mechanical Engineering from the Government College of Engineering and ME in Internal Combustion Engine at the Anna University. Her research interests lie in the area of internal combustion engines, renewable energy resources and heat transfer ranging from theory to design to implementation. In recent years, she has focused on better techniques for expressing, analysing, and executing real time projects.

This paper is a revised and expanded version of a paper entitled 'Transient effect of indoor heat generation on a closed room' presented at 3rd International Conference on Bioenergy, Environment and Sustainable Technologies, Tiruvannamalai, 23–25 January 2017.

1 Introduction

The building solar radiation waves are classified into two types there are short waves and long waves. When a short wave reaches the building wall, partial radiation reflects to the environment and some part if waves stored in the wall. By continuous solar radiation strike the building wall along with long wave which increases the external wall temperature and it increases the outdoor air temperature. The solid wall conducts the heat energy through the mode of conduction and by this means it transfers the heats to the internal surface of the building. The hot internal surface of the building warm up the indoor air (indoor air typically at lower temperature than the outdoor air during day time) by convection (Mao et al., 2017).

The productivity and good health of a human is depends on the good indoor air quality. For maintaining the indoor air quality 40% of total energy is consumed all around the world in building sector. Building space load is the component used for building space heating/cooling depends on outdoor climatic conditions and indoor conditions like internal heat, moisture and building walls (Harish and Kumar, 2016). An attempt made to thermal energy storage was to restrict the heat flow through the wall and the roof with phase change material (PCM) panels installed at the external surface of the building wall and roof in the view of improving the indoor thermal comfort (Kong et al., 2014). For the building cooling, the tree shade analysis has performed with long and small tree. The solar radiation is reduced by the tree shade. The closer and taller trees reduced the external wall temperature up to 9°C (Berry et al., 2013).

The commercial wind tower of a room was analysed under wind driven and buoyancy driven flow arrangements with internal heat source and window opening position. The study presents that, primary driving force is wind and the buoyancy is the secondary. When implementing internal heat source along with the window openings enhances the buoyancy driven ventilation of the commercial building (Hughes and Cheuk-Ming, 2011). The localised transient floor level internal heat generation was modeled as a room with three layer of buoyancy flow in near ceiling layer, middle layer and lower layer. When the vent is small the near ceiling layer is small and the middle layer is larger, with increase in time the middle layer increases gradually. The buoyancy flow is depends on the time, internal heat flux, floor area and room enclosure height (Yang et al., 2013).

Transient natural ventilation of buoyancy driven point heat source pre heated room was investigated. The thermal turbulence plume typical warm air from a point heat source rises to the roof, weaker thermal plume break off the thicker flow region as suspend (Fitzgerald and Woods, 2010). Buoyancy driven natural ventilation simulation was performed with symmetrical and non-asymmetrical cavities with side and vertical openings. The heating of the wall by solar radiation is turbulence and the RNG k- ϵ turbulence was employed for the numerical simulation in computational fluid dynamics (CFD) package FLUENT. Heated wall region air propel the higher air velocity in the cavity was found (Gan, 2010). The air flow pattern of an isolated room with fixed thermal boundary conditions was performed with real time measured building element (floor, wall and roof) temperatures during summer (Prakash and Ravikumar, 2015). Solar assisted numerical study on an atrium building performance was investigated under various design parameters based on its geometry using CFD solver fluent (Hussain and Oosthuizen, 2012). The buoyancy driven day and night time numerical simulation were performed and the results are presented on the parameters effecting on the indoor comfort was air flow pattern, air flow rate and temperature distribution. The results presented that internal heat generation is inadequate and the outdoor climatic conditions were most significant factor. The building height is another important factor which influences the buoyancy effect (Hussain and Oosthuizen, 2013). The under floor air distribution of a high ceiling numerical analysis were demonstrated that the flow field of air velocity and temperature distribution within the space by means of thermal stratification (Kim et al., 2013). In natural convection a single heat source induces the thermal plume in three dimensional analysis (Hernandez, 2015). Without any stack effect the indoor heat source creates the thermal plume inside the room which fills the low density hot air within the space by mixing up the hot and cold region. The region of cold and hot air is unstable. The gravitational force direct the propagation of the thermal plume and initial formulation of plume, based on the density of air, heat source and time (Ji et al., 2015). It is also reported that the space heating numerical simulation were carried out through wall and floor heating. Thermal stratification exists during wall heating of the room (Karabay et al., 2013). Indoor air velocity is less than 0.2 m/s mostly and the indoor occupant body heat is the important factor in the flow region (Ge et al., 2013).

Transient natural ventilation investigation was performed on vented room with localised floor level heat source considered for the experiment. The indoor air temperature on different pole were discussed nearer and far away to the vent arrangements under various indoor and outdoor ambient conditions (Yang et al., 2014). Another numerical simulation was conducted on transient flow development of natural ventilated building room with floor level point various range of heat source. The results shows that internal heat load, vent area and indoor air temperature plays the significant effect on the transient behaviour (Yang et al., 2015).

So far many research attempts made to improve the indoor air cooling or heating for hot and cold climatic regions. But indoor air temperature is hike under transient condition with various range of internal indoor heat generation rate and its maximum indoor air temperature is essential to select the most appropriate technique and technologies are suitable to reduce or increase the air temperature dependent on the climatic conditions. This work aimed to address the transient effect of closed room indoor air temperature and velocity distribution under constant thermal boundary conditions.

2 Model description

Based on the building construction the types of rooms were classified as sun light exposure and non exposure. In this work a single floor building has two different rooms such as no walls sunlight exposure and two walls sun light exposure are taken for this work. Since the building is a single floor, the roof of the two rooms are sun light exposure one. The dimensions of the rooms are similar for the both the case having $5\text{m} \times 5\text{m} \times 5\text{m}$ was considered for the grid based numerical simulation, separately. In general room elements are floor, four side walls and roof. Sun light exposure wall room has two hot walls and two cold side walls on the other hand the non exposure case has all four walls are cold walls only.

Figure 1 Schematic illustration of room model (a) indoor measuring pole location (b) measuring point on a pole

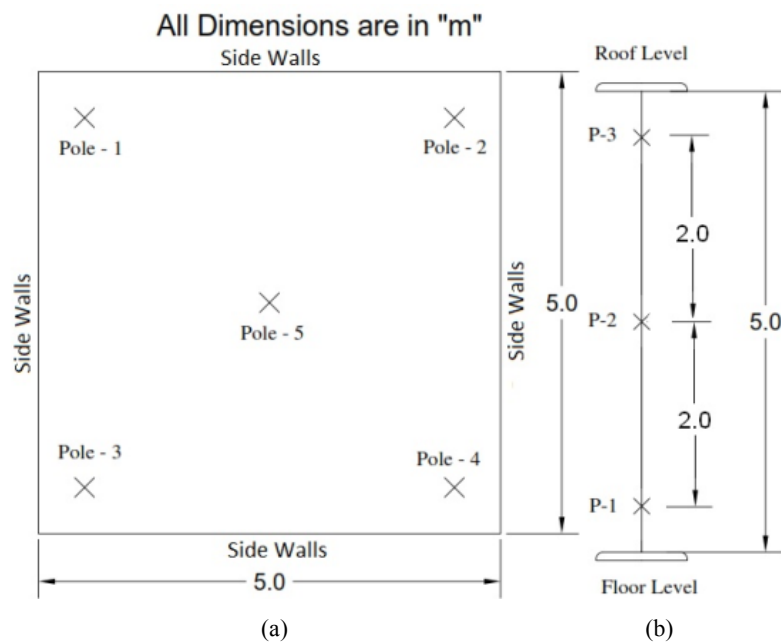


Figure 1(a) shows the schematic illustration of room model top view of the indoor measuring pole location. Totally five poles named as pole-1, pole-2, pole-3, pole-4 and pole-5. Pole-1, pole-2, pole-3 and pole-4 was located nearer to the corner of the side wall junctions, where the distance of the measuring poles were 0.75m from both walls. The central pole-5 located at exact centre of the room. Figure 1(b) shows the location of measuring point on a single pole. The measured points are located at 0.5m, 2.5m and 4.5 m from the floor level of the all poles. Case 1: All walls are cold walls, Case 2: Two walls are considered as hot walls. The hot wall junction measuring pole is pole-4 and the cold wall measuring pole is pole-1. The rest of the poles pole-2 and pole-3 are located at the junction where the hot and cold walls connect together. The localised indoor heat liberation by the indoor elements was assigned to the floor which is varied from 0 W/m^2 (no heat generation), 5 W/m^2 , 15 W/m^2 and 25 W/m^2 . The room is considered as closed and perfectly sealed.

3 Numerical scheme

The model was generated and the grid independent study has been performed to predict the accurate results of the simulation. The various grid densities of 9,033, 29,443, 68,453 and 132,063 were tested and the finer grid densities of 68,453 and 132,063 shows the most similar indoor temperature values, where the difference in temperature is 0.08°C , so the grid density 68,453 elected for further simulations. The CFDs tool the finite volume solver ANSYS-Fluent is used to perform this numerical simulation. The mass, momentum and energy equations are central difference scheme; quick scheme and k- ϵ turbulence model are selected respectively. The room element temperatures are considered as 303K for floor, 312K for cold walls and 325K for hot walls and roof, the initial indoor air temperature is 306K. The indoor air properties are considered as constant throughout the simulation except density. Initial indoor air density is taken as 1.225 kg/m^3 under boussinesq approximation with thermal expansion of 0.003. For solution control, second order upwind method is used and the convergence criteria fixed for the numerical simulation is 10^{-4} .

4 Results and discussion

The numerical study has been performed on different parameters of a room with different side wall conditions and various internal heat generation rates. The results of the various cases are discussed below.

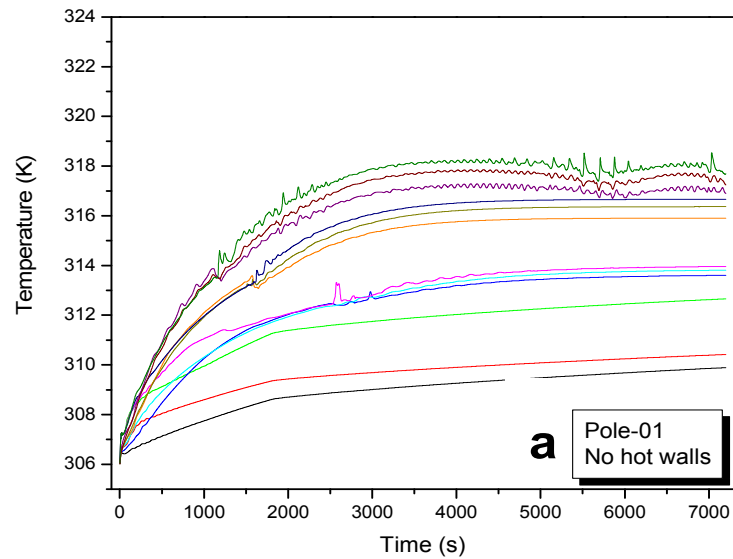
4.1 Case 1: walls non exposure to sunlight (without hot walls)

Figure 2(a) and 2(c) shows pole-1 transient effect of indoor air temperature and velocity profile of no hot walls case. In this case without internal heat generation, the indoor air temperature rises gradually. After the simulation period of 7,200s the temperature difference among the measured point is markable. At different measured point on this location (pole-1), lower level measured point shows the least air temperature and higher level measured point shows the higher air temperature which is 309.88°C , 310.42°C and 312.65°C at lower (0.5 m level), middle (2.5 m level) and top (4.5 m level) respectively. This is due to the boundary of the room elements temperature increases the air temperature. The increase in air temperature at the region of side walls reduces the air density and the change in air density produces the buoyancy effect, the low density warm air will move towards top of the room and the cold air at high density flows from higher level to lower level.

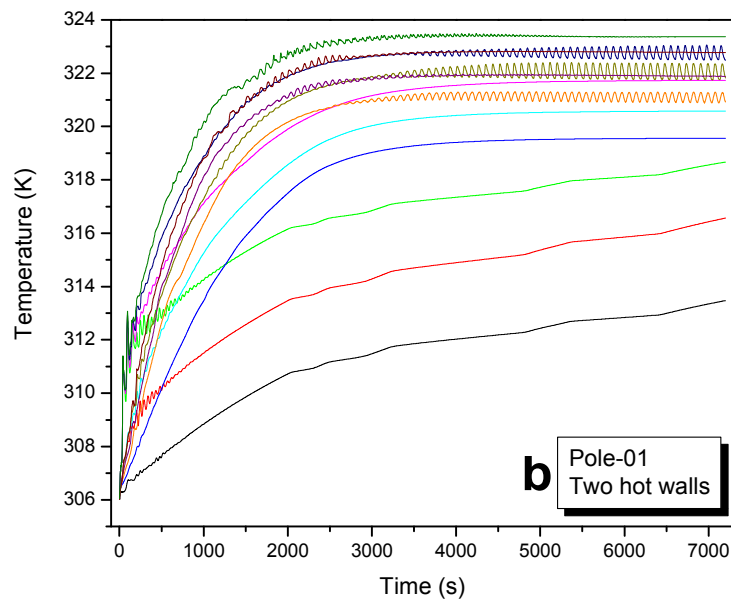
The velocity profile shows the initial fluctuation on indoor velocity during initial period of time. This is because of difference in indoor air temperature of the side walls make the wall region air as warmer nearer to the wall. The sudden change of air density initiates air movement towards top of the room. The replacement of the warm by the cold air is rapid during initial period of time. When increase in time period the fluctuations reduced further and it attains steady. The higher velocity found at lower level and the lower velocity noted at top level of the room. In top level the movement of air is low, due to the existence of warm air slow down the velocity of the indoor and it makes it as constant over the time period. Temperature profile at other poles (Pole-2, pole-3, pole-4

and pole-5) are similar to each other which is showing Figures 3, 4, 5 and 6(a). Figures 3, 4 and 5(c) shows the velocity profile pole-1, 2, 3 and 4 same values except pole-5.

Figure 2 Transient effect of indoor air pole-1 on various range of internal heat generation, (a) no hot walls temperature profile (b) two hot walls temperature profile (c) no hot walls velocity profile (d) two hot walls velocity profile (see online version for colours)

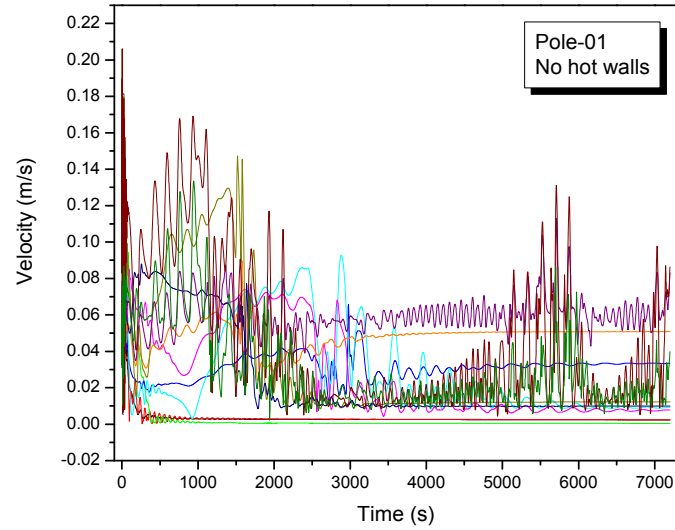


(a)

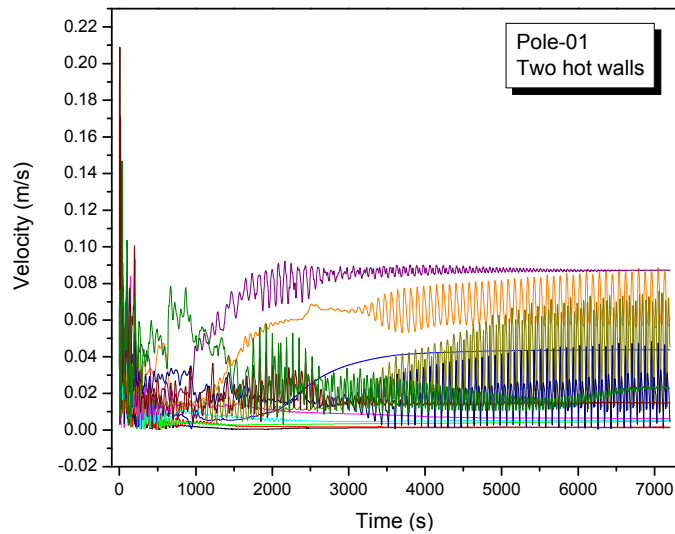


(b)

Figure 2 Transient effect of indoor air pole-1 on various range of internal heat generation, (a) no hot walls temperature profile (b) two hot walls temperature profile (c) no hot walls velocity profile (d) two hot walls velocity profile (continued) (see online version for colours)



(c)



(d)

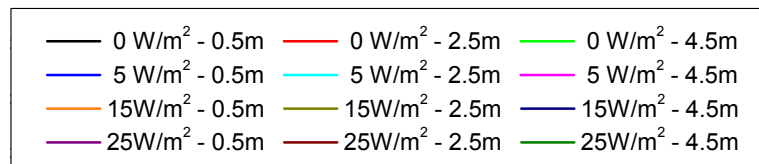
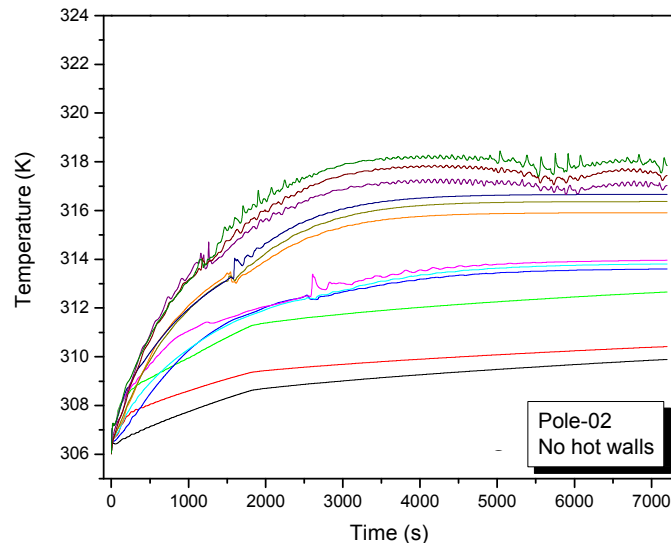
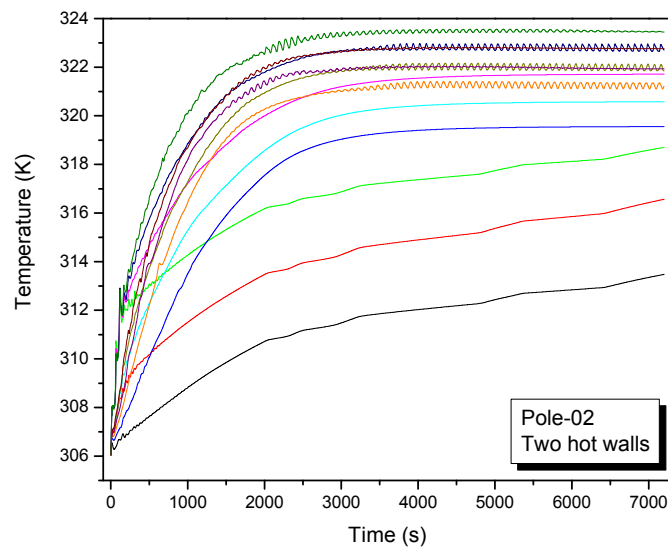


Figure 6(c) shows the wide range of fluctuation in than other measuring points, this is due to the location of pole-5 is mid of the room. Initial movement of warm air from the side wall region travel to top of the room and its volume increase with increase in time. Combined air movement of high density air moves towards floor and the low density warm air moves upward creates the horizontal filling makes this pole-5 as more fluctuating than the other measuring poles.

Figure 3 Transient effect of indoor air pole-2 on various range of internal heat generation, (a) no hot walls temperature profile (b) two hot walls temperature profile (c) no hot walls velocity profile (d) two hot walls velocity profile (see online version for colours)

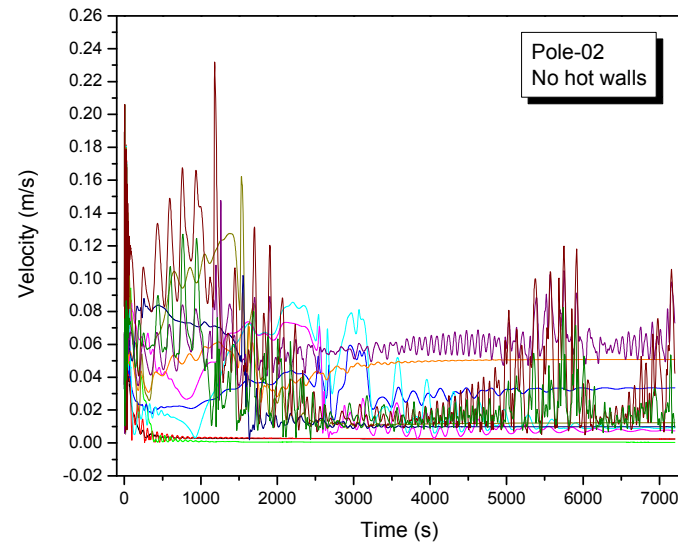


(a)

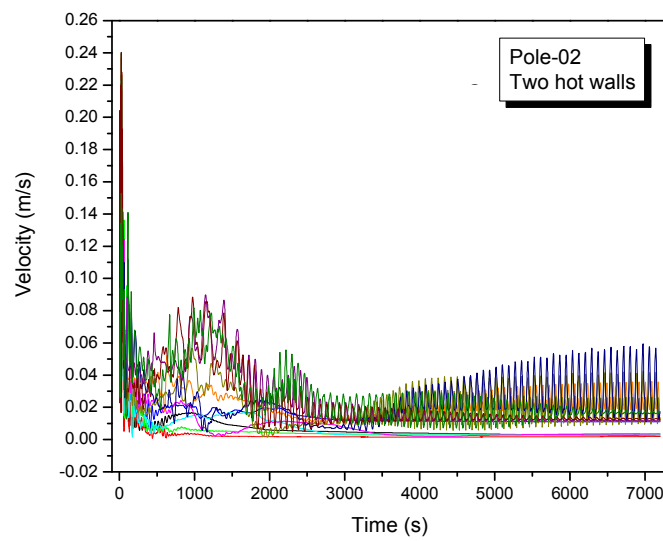


(b)

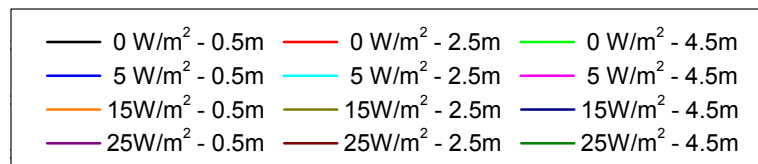
Figure 3 Transient effect of indoor air pole-2 on various range of internal heat generation, (a) no hot walls temperature profile (b) two hot walls temperature profile (c) no hot walls velocity profile (d) two hot walls velocity profile (continued) (see online version for colours)



(c)



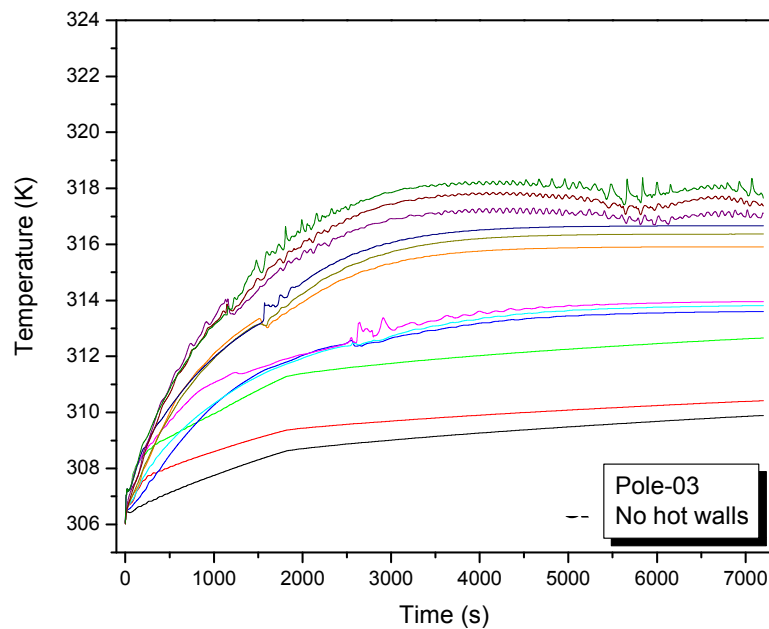
(d)



When introducing the internal heat flux was 5 W/m^2 to the same volume of the room with same boundary conditions, the indoor air temperature increases further. The rate of change of indoor air temperature is higher at initial time period; the temperature increase rate reduces with increase in temperature and time. Initially the temperature difference exists among the measuring points in all poles. The lower measuring points shows the lower air temperature and higher measuring points shows the higher temperature at all poles. The time of 2,746 seconds the temperature among the measuring points are very close together. This point is called as stable point, where the temperature among the pole is same. Later the time period 2,746 second except pole-5 the same trend is followed in uniform temperature differences as shown in Figures 2, 3, 4 and 5(a).

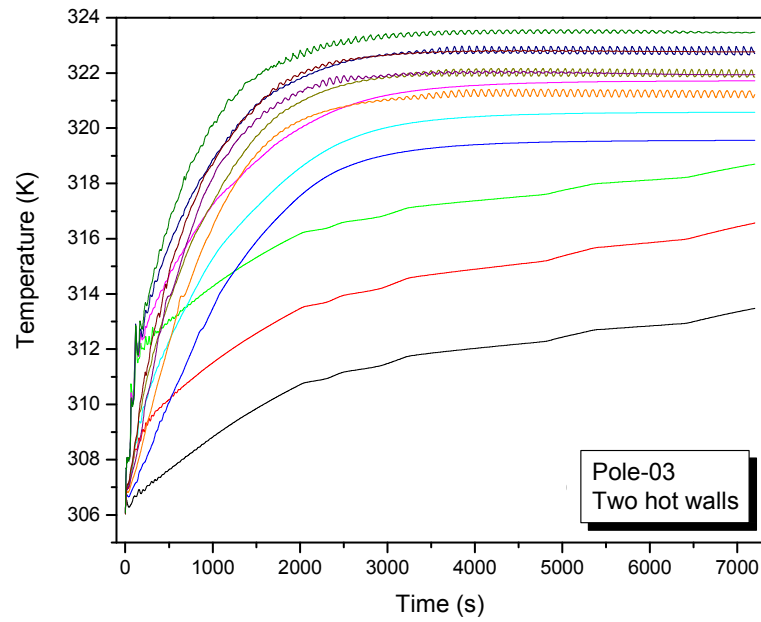
On pole-5 the lower level measuring point shows the higher temperature than the higher level measuring point. This is due to the formulation of thermal plume core at high temperature produced by the internal heat flux travel towards top of the room makes the lower region as hotter than the top region. The travel of thermal plume mixed with the indoor air and increase the warm air formation rate in additional to the room enclosures (side walls and roof) which is shown in Figure 6(a). The velocity profile for the 5 W/m^2 , initial velocity is higher at top level and after the stable point lower level measuring point show the higher velocity except pole-5 which is shown in Figures 2, 3, 4 and 5(c) for the reason that till the stable point room elements (side walls and roof) leading the heating process of indoor air thereafter internal heat flux playing the role.

Figure 4 Transient effect of indoor air pole-3 on various range of internal heat generation, (a) no hot walls temperature profile (b) two hot walls temperature profile (c) no hot walls velocity profile and (d) two hot walls velocity profile (see online version for colours)

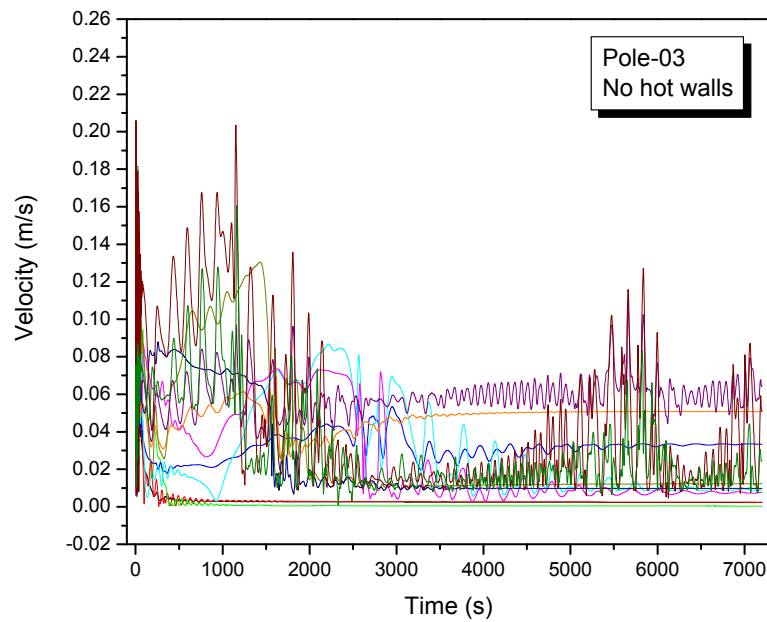


(a)

Figure 4 Transient effect of indoor air pole-3 on various range of internal heat generation, (a) no hot walls temperature profile (b) two hot walls temperature profile (c) no hot walls velocity profile and (d) two hot walls velocity profile (continued) (see online version for colours)

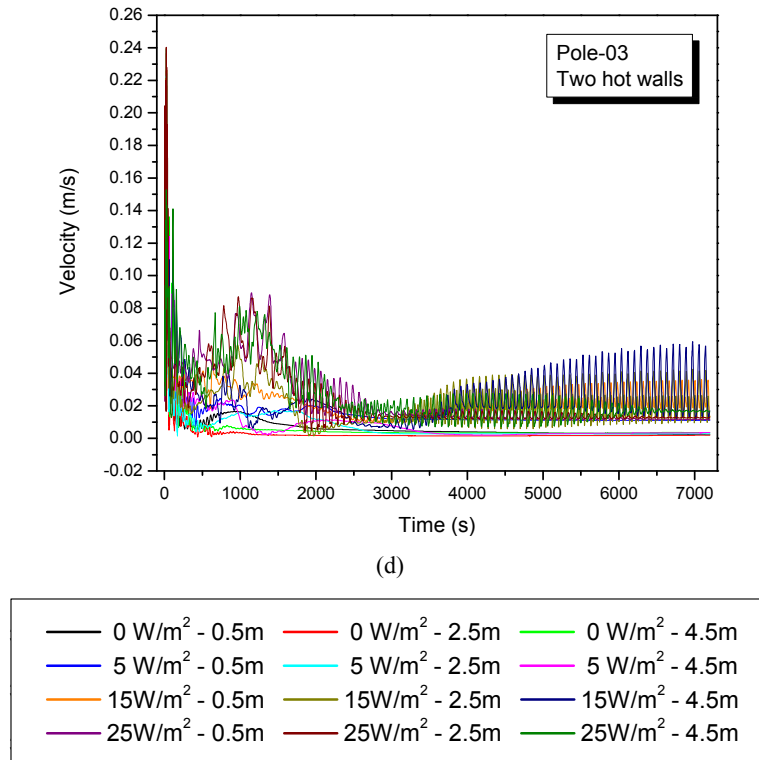


(b)



(c)

Figure 4 Transient effect of indoor air pole-3 on various range of internal heat generation, (a) no hot walls temperature profile (b) two hot walls temperature profile (c) no hot walls velocity profile and (d) two hot walls velocity profile (continued) (see online version for colours)

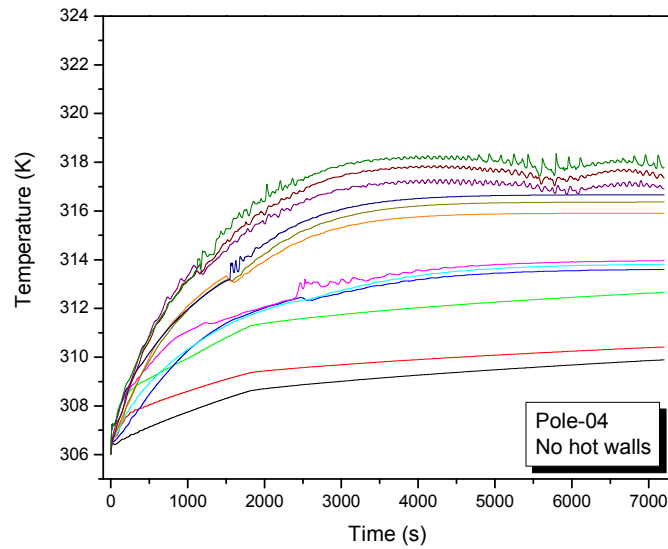


So the maximum velocity found at lower level of the room after stable point. At pole-5, initial velocity is much lower at all three measuring points, after reaching stable point the velocity propelled. Since the thermal plume formulation and stratified flow increases the velocity of the air at middle of the room till room top. The shape of the velocity fluctuation after stable point is sinusoidal cone. The fluctuation reduces with increase in time by filling the warm air within the volume. The air velocity is in the higher order of the pole-5 is middle 2.5m level, lower 0.5m level and 4.5 m level at top as shown in Figure 6(c). At the end of 7200 seconds simulation the velocity noted as 0.155m/s, 0.113m/s and 0.036m/s for middle, lower and higher level respectively.

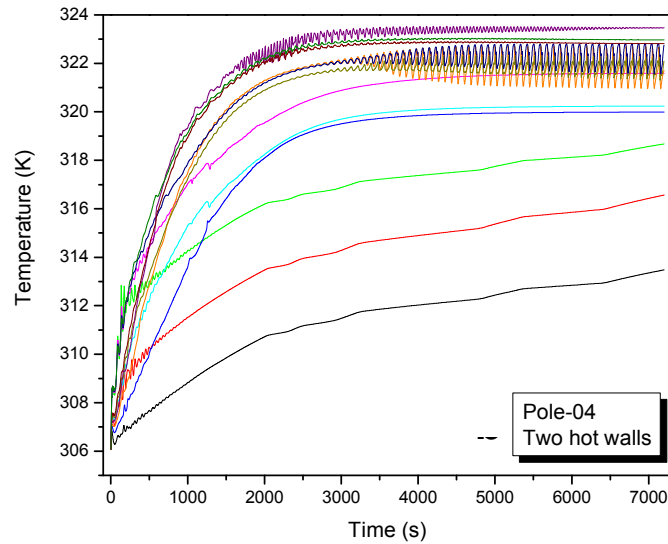
Increase in internal heat source from 5 W/m² to 15 W/m², the trend follows by the 15 W/m² is same as 5 W/m². But the variations found at stable point, where it occurs at 1,646 seconds. The variation of stable point is earlier than that of lower heat generation rate and the different level temperatures are higher than the previous case (5 W/m²) it is noted as 314.45°C which 1.8°C greater than lower. In pole-5 at stable point the thermal plume starts formed earlier than the 5 W/m² case and due to the higher heat flux the lower level measuring point shows the higher temperature among the region of flow. Initially slight temperature fluctuation found at lower region with increase in trend. The steady temperature state prevails at 4,527 seconds. After reaching steady state the difference in temperature is found with lower (316.42°C) to middle level and top level

measuring points are found as 0.09°C and 1.58°C respectively. At the end of 7,200 seconds simulation the rise in indoor air temperature at various increases with internal heat flux ranging from 0 W/m^2 to 25 W/m^2 . The increase in air temperature from base case 0 W/m^2 to 25 W/m^2 is 19.19% to 8.62%, 18.25% to 9.08% and 12.73% to 3.30% at 0.5m level, 2.5 m level and 4.5 m level respectively.

Figure 5 Transient effect of indoor air pole-4 on various range of internal heat generation, (a) no hot walls temperature profile (b) two hot walls temperature profile (c) no hot walls velocity profile (d) two hot walls velocity profile (see online version for colours)

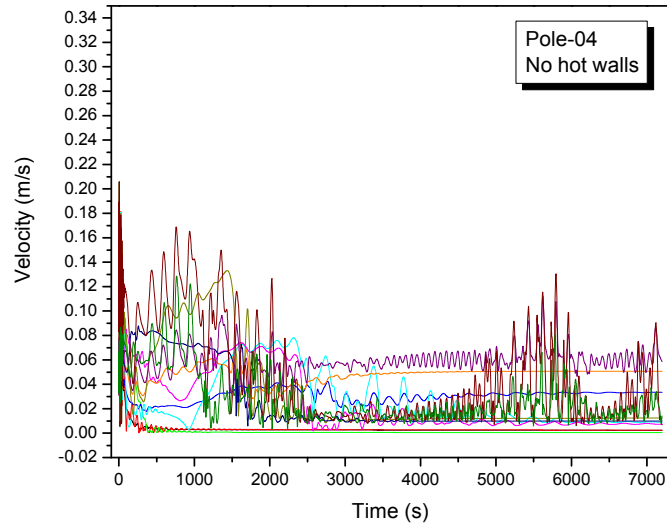


(a)

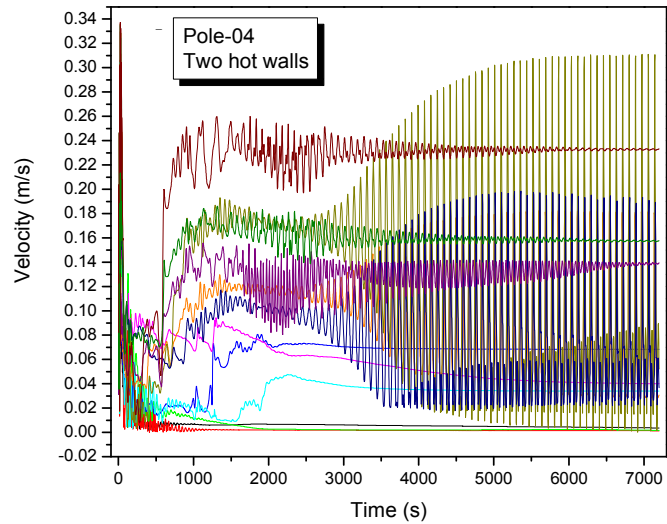


(b)

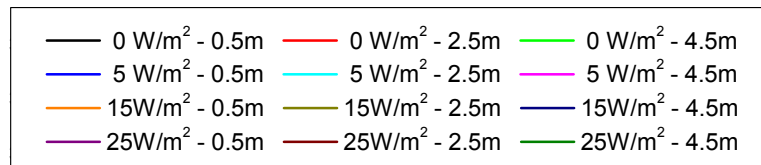
Figure 5 Transient effect of indoor air pole-4 on various range of internal heat generation, (a) no hot walls temperature profile (b) two hot walls temperature profile (c) no hot walls velocity profile (d) two hot walls velocity profile (continued) (see online version for colours)



(c)

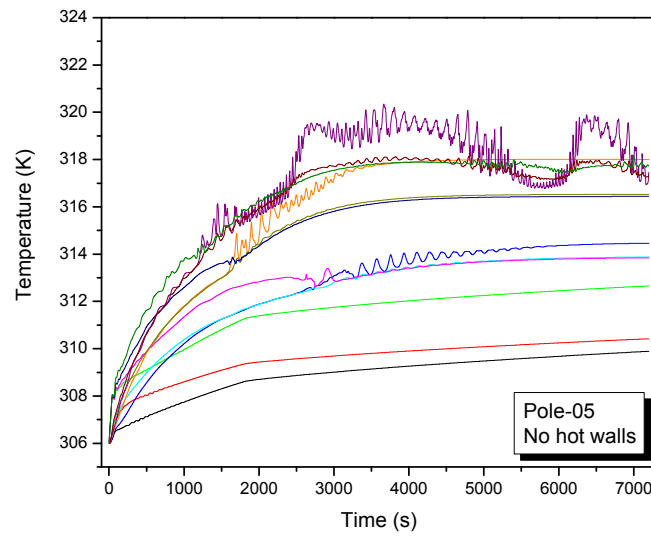


(d)

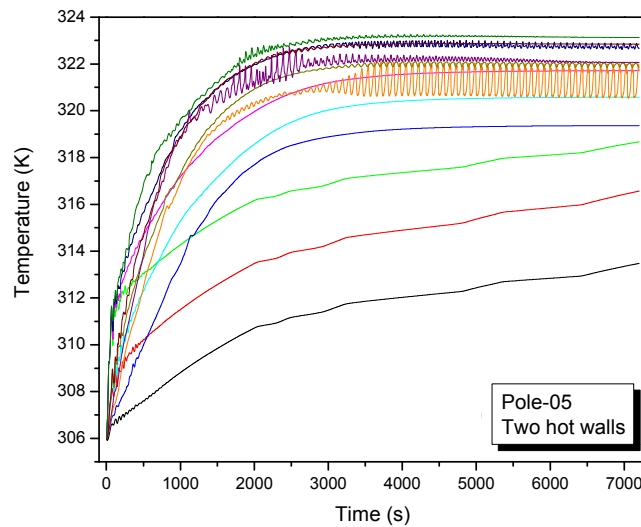


During this state the air velocity at pole-5 reaches its constant velocity and it varies in the range of 0.156m/s, 0.113m/s and 0.036m/s for middle level, lower level and higher level respectively. For the case of 25W/m^2 the stable point occurs earlier than the 15W/m^2 where the time is noted as 1187 seconds. Afterward it is noted that there is slight temperature fluctuation in all level measuring points and poles. The fluctuations are uniform among pole-1, 2, 3 and 4 nevertheless pole-5 after stable point the lower level measuring point shows the maximum variation time to time.

Figure 6 Transient effect of indoor air pole-5 on various range of internal heat generation, (a) no hot walls temperature profile (b) two hot walls temperature profile (c) no hot walls velocity profile (d) two hot walls velocity profile (see online version for colours)

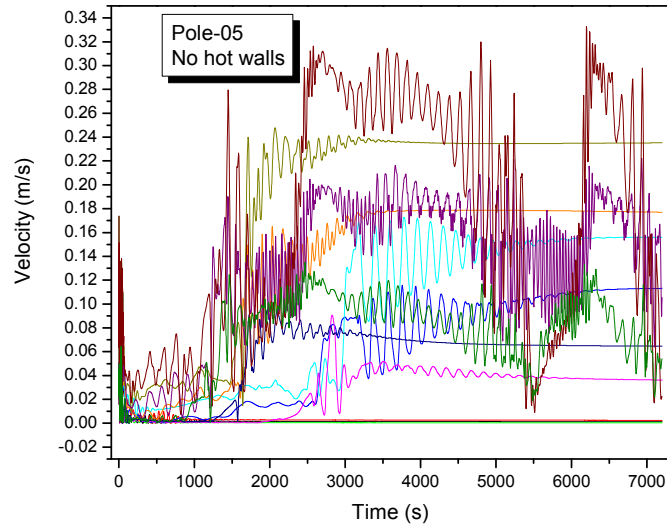


(a)

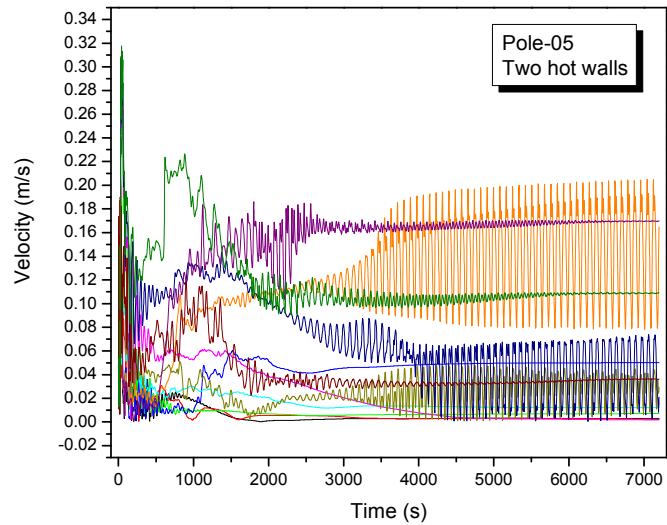


(b)

Figure 6 Transient effect of indoor air pole-5 on various range of internal heat generation, (a) no hot walls temperature profile (b) two hot walls temperature profile (c) no hot walls velocity profile (d) two hot walls velocity profile (continued) (see online version for colours)



(c)



(d)

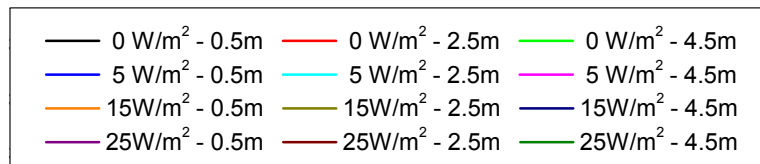
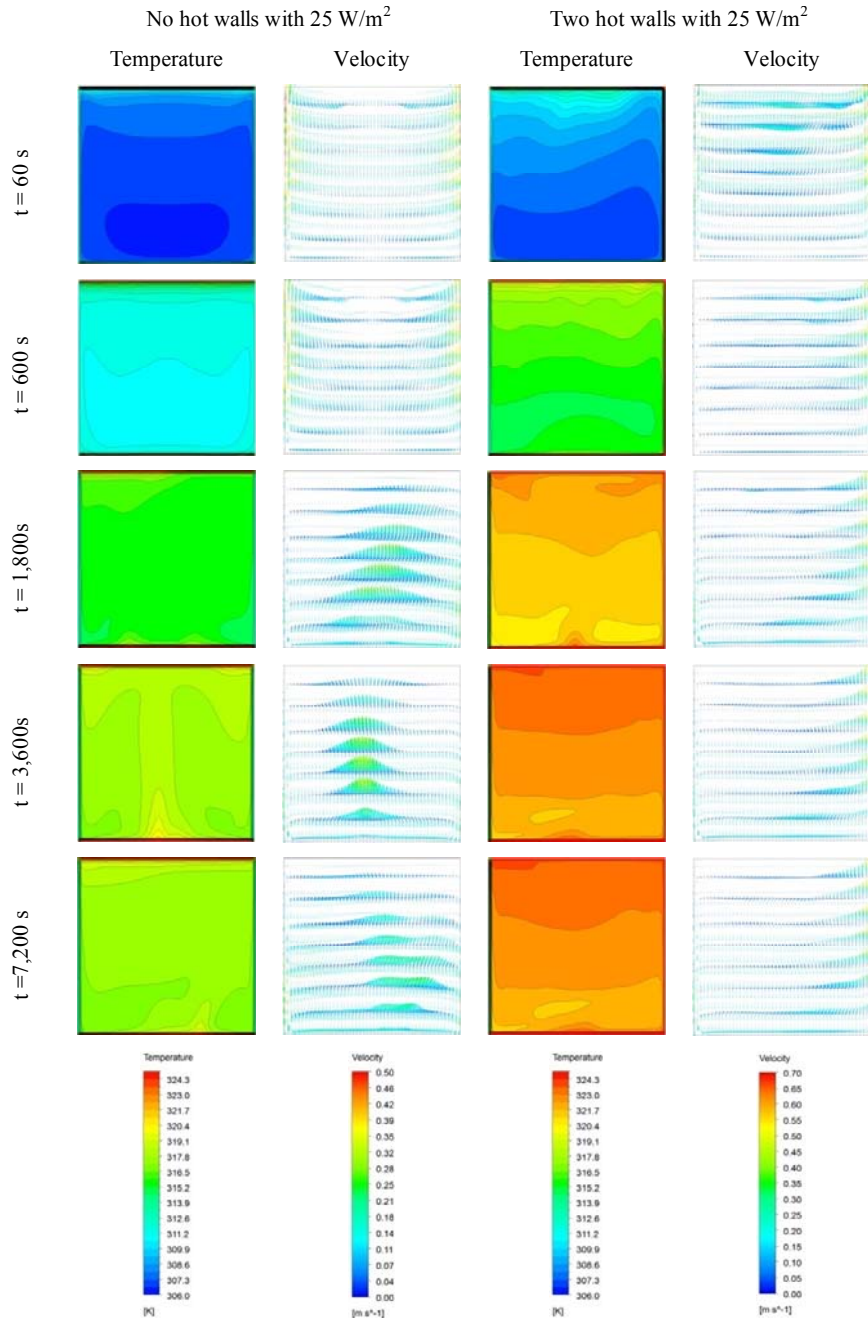


Figure 7 Air temperature and velocity profile with internal heat generation of 25 W/m^2 (see online version for colours)



This is due to the thermal plume swings higher in order with higher indoor air temperature filled maximum over the volume. Thus the maximum indoor air temperature noted at lower level where the temperature of the air is 320.34°C . Accordingly the

velocity of the measuring pole-5 varies with respect to plume swing where the maximum velocity found at middle level of the room as 0.332m/s rest of the level velocity is lower than 0.332m/s velocity.

4.2 Case 2: two side walls open to sunlight (two hot walls)

The transient effects of indoor air temperature and velocity profile with two hot walls are shown in Figures 2, 3, 4, 5, 6(b) and 6(d). The effect of walls temperature increases the air temperature nearer to the wall region. Due to the change in temperature variation in indoor air temperature the buoyancy effect drive the warm air flows towards top of the room. Initially the pole-4 top level measuring points observes more temperature fluctuation among all measuring points. This is due to the two hot wall junctions at the surface temperature of 325K, begins the flow and it reaches the top level. Then the warm air horizontal flow fill the top level and at the same time the hot junction low density warm air replaced by the cold air by transport of the air molecules makes the initial air temperature fluctuation at top level. The subsequent movement of air makes the region as more fluctuation. The pole-1 also noted same kind of fluctuations, which indicates that after reaching the warm air at pole-4 region the horizontal flow of warm air to cold junction it makes the fluctuation at cold junction measuring pole-1.

Temperature and velocity profile of the pole-2 and pole-3 are similar, since the cold and hot side wall junction exists at this location. For this case, the surface of the room and internal heat source heats the indoor air so rapidly, hence the formulation of stable temperature over the volume is not a stable one. The formulation of thermal plume is so early since the building enclosures heats the indoor air, but the hot walls stratifies flow as a result the vertical plume is pulled towards the hot wall side. Initial stage of the transient simulation of all range of internal heat flux rate with two hot walls case, the maximum temperature and velocity noted at pole-4 location in middle level or top level measuring point. The maximum velocity of 0.337 m/s found at pole-4 middle level measuring point. Furthermore higher velocity may occur at the extreme hot junctions. In pole-4 Figure 5(d) more velocity fluctuations noted at middle level measuring point with 15W/m² heat flux, which indicates the availability of unstable thermal plume and the same point there is no longer fluctuations found with 25W/m² heat flux. The maximum indoor air temperature is noted as 323.46°C which is highest ever in the measuring points measured at pole-4 top level. With increase in indoor heat flux 0 W/m² to 25 W/m², the maximum air temperature after 7200 seconds of simulation is varies from 20.78% to 15.04% at 0.5m level. At 2.5m level and 4.5m level the maximum temperature variations are noted 14.23% to 9.18% and 10.29% and 6.85% respectively.

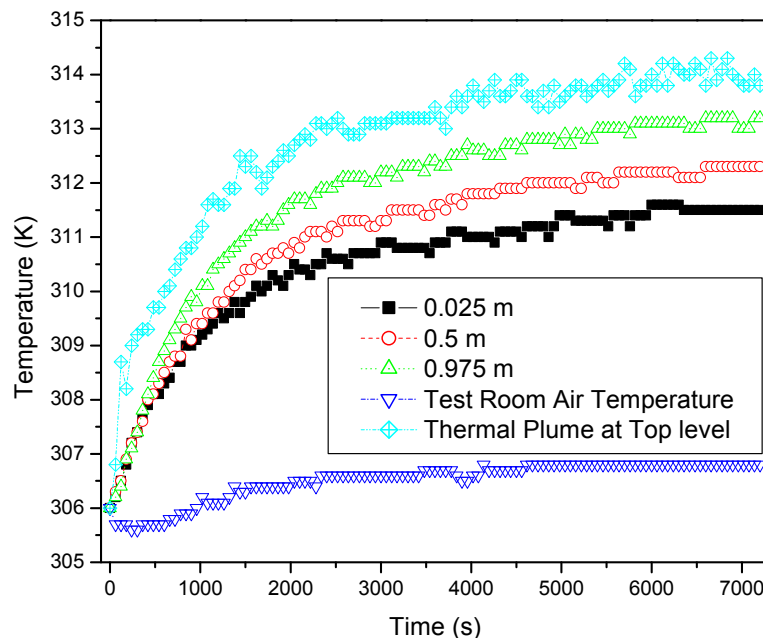
The transient temperature profile and velocity vector of indoor air is shown in Figure 7. The cross sectional area plots are captures at centre of the room (on XZ plane at 2.5 m from Y direction side walls) with internal heat flux of 25 W/m². From which it is clear that with no hot walls case the initial air movement is induced by the side wall temperatures, which is uniform for all four side walls. The maximum air velocity found nearer to the side walls during initial time period. Later when the uniform temperature reaches throughout the indoor air volume the thermal plume forms and it leads the air movement majorly at the centre of the room. After formulation of the thermal plume, for the maximum indoor air temperature found at the centre of the room for no hot wall case. Whenever two hot walls exists the flow initiates by the two hot walls so that indoor air temperature reaches maximum temperature soon compared to no hot wall case. The

higher velocity of the indoor air is found at nearer to the hot surface all the time. Comparing to the no hot wall case and hot wall case thermal plume is no longer effective, since the thermal plume was attracted by the air movement of the hot side walls. So the vertical temperature at various levels is increasing by increase in height from floor level. The maximum temperature within the model after 7,200 seconds is 319.89 K for no hot wall case and 323.14 K for hot wall case.

5 Model validation

A scale down reduced model experimental setup was made with 12 mm plywood containing volume of 1 m^3 (one metre on each side). The room model was constructed with door and window. A localised heat source of 100 W placed at the floor level of the room model and indoor air temperature measuring points were located at ground level (0.025 m), middle level (0.5 m), top level (0.975 m) and top of the thermal plume (0.975 m) at room centre. This setup was kept at a test room whose temperature also measured. At constant floor, wall and roof temperature, the room model was closed and the heat source was turned ON. The temperatures were measured with resistance temperature detectors (RTD) connected to the data logger at the time interval of 60 seconds over the period of 7,200 seconds. The accuracy of the RTD is $\pm 0.1^\circ\text{C}$.

Figure 8 Experimental validation of transient indoor air temperature distribution (see online version for colours)



The Figure 8 shows the transient temperature distribution of indoor air. The transient indoor air temperature increases with increase in time, the lower to the higher indoor air

temperature is in the order of lower level, middle level and top level. The thermal plume temperature shows the maximum over the time period which is measure as 314.3 K as maximum. The minimum indoor air temperature found at lower level of the room which is 311.5 K. The results of the experimental validation shown in Figure 8, the trend and temperature distribution at different location of indoor air under constant internal heat generation with no hot walls were similar as compared to the CFD simulation as shown in Figure 7. So there is a good agreement among CFD simulation results and experimental results under same conditions.

In general with the above study, the predicted accuracy of the numerical simulation for the unsteady flow development of a closed room confirm that CFD simulation employed in this study is capable of flow characteristics and temperature distribution satisfactorily.

6 Conclusions

Based on the results of transient flow numerical simulation in two cases with hot walls and without hot walls under various range of internal heat generation are summarised below.

Without any hot walls and internal heat generation, the increase in indoor air temperature is time-consuming when compared to internal heat generation. The room element and the internal heat generation rises the indoor air temperature, whenever the indoor air temperature reaches the stable temperature throughout the volume, the thermal plume is propagates. The stable thermal plume was occurs at centre of the room, when increase in heat flux the stable plume is swings. The rate of increase in temperature decreases with increase in time. In two hot walls without internal heat generation, increase the air temperature more rapid. While increase in small heat flux of 5 W/m^2 increases the air temperature rapidly and further increment in heat flux 15 W/m^2 and 25 W/m^2 promotes the maximum indoor air temperatures slightly higher than the earlier. So the maximum indoor air temperature noted at ploe-4 top level measuring point where the two hot walls are joined together.

In internal heat flux increases the indoor air temperature. The temperature rise is depends on the building enclosures and internal heat source. The maximum indoor air temperature is noted with 25 W/m^2 at 0.5m level and 5 W/m^2 at 4.5 m level. For no hot wall case the maximum and minimum percentage of temperature rise is estimated as 19.19% and 3.3%, intended for two hot wall case 20.78% and 6.85% respectively.

This transient numerical simulation shows that, the maximum indoor air temperature is dependent on magnitude of internal heat flux, building enclosure temperatures and initial indoor air temperature. The flow pattern and the warm region of the room were differed with the internal heat generation and hot side walls. Therefore, before choose the space cooling technique or equipment the physical condition of the building is essential to analyse according to its environment.

References

- Berry, R., Livesley, S.J. and Aye, L. (2013) 'Tree canopy shade impacts on solar irradiance received by building walls and their surface temperature', *Building and Environment*, Vol. 69, No. 1, pp.91–100.
- Fitzgerald, S.D. and Woods, A.W. (2010) 'Transient natural ventilation of a space with localised heating', *Building and Environment*, Vol. 45, No. 12, pp.2778–2789.
- Gan, G. (2010) 'Simulation of buoyancy-driven natural ventilation of buildings – impact of computational domain', *Energy and Buildings*, Vol. 42, No. 8, pp.1290–1300.
- Ge, Q., Li, X., Inthavong, K. and Tu, J. (2013) 'Numerical study of the effects of human body heat on particle transport and inhalation in indoor environment', *Building and Environment*, Vol. 59, No. 1, pp.1–9.
- Harish, V. and Kumar, A. (2016) 'A review on modeling and simulation of building energy systems', *Renewable and Sustainable Energy Reviews*, Vol. 56, No. 1, pp.1272–1292.
- Hernandez, R. (2015) 'Natural convection in thermal plumes emerging from a single heat source', *International Journal of Thermal Sciences*, Vol. 98, No. 1, pp.81–89.
- Hughes, B.R. and Cheuk-Ming, M. (2011) 'A study of wind and buoyancy driven flows through commercial wind towers', *Energy and Buildings*, Vol. 43, No. 7, pp.1784–1791.
- Hussain, S. and Oosthuizen, P.H. (2012) 'Numerical investigations of buoyancy-driven natural ventilation in a simple atrium building and its effect on the thermal comfort conditions', *Applied Thermal Engineering*, Vol. 40, No. 1, pp.358–372.
- Hussain, S. and Oosthuizen, P.H. (2013) 'Numerical investigations of buoyancy-driven natural ventilation in a simple three-storey atrium building and thermal comfort evaluation', *Applied Thermal Engineering*, Vol. 57, No. 1, pp.133–146.
- Ji, J., Li, M., Li, Y., Zhu, J. and Sun, J. (2015) 'Transport characteristics of thermal plume driven by turbulent mixing in stairwell', *International Journal of Thermal Sciences*, Vol. 89, No. 1, pp.264–271.
- Karabay, H., Arıcı, M. and Sandık, M. (2013) 'A numerical investigation of fluid flow and heat transfer inside a room for floor heating and wall heating systems', *Energy and Buildings*, Vol. 67, No. 1, pp.471–478.
- Kim, G., Schaefer, L., Lim, T.S. and Kim, J.T. (2013) 'Thermal comfort prediction of an underfloor air distribution system in a large indoor environment', *Energy and Buildings*, Vol. 64, No. 1, pp.323–331.
- Kong, X., Lu, S., Li, Y., Huang, J. and Liu, S. (2014) 'Numerical study on the thermal performance of building wall and roof incorporating phase change material panel for passive cooling application', *Energy and Buildings*, Vol. 81, No. 1, pp.404–415.
- Mao, A., Luo, J. and Li, Y. (2017) 'Numerical simulation of thermal behaviors of a clothed human body with evaluation of indoor solar radiation', *Applied Thermal Engineering*, Vol. 117, No. 1, pp.629–643.
- Prakash, D. and Ravikumar, P. (2015) 'Analysis of thermal comfort and indoor air flow characteristics for a residential building room under generalized window opening position at the adjacent walls', *International Journal of Sustainable Built Environment*, Vol. 4, No. 1, pp.42–57.
- Yang, X., Kang, Y. and Zhong, K. (2013) 'Theoretical modeling of unsteady buoyancy-driven natural ventilation', *HVAC&R Research*, Vol. 19, No. 2, pp.148–158.
- Yang, X., Zhong, K., Kang, Y. and Tao, T. (2015) 'Numerical investigation on the airflow characteristics and thermal comfort in buoyancy-driven natural ventilation rooms', *Energy and Buildings*, Vol. 109, No. 1, pp.255–266.
- Yang, X., Zhong, K., Zhu, H. and Kang, Y. (2014) 'Experimental investigation on transient natural ventilation driven by thermal buoyancy', *Building and Environment*, Vol. 77, No. 1, pp.29–39.